

## Enhanced visible light photocatalytic activity of AgI/TiO<sub>2</sub> composite fabricated by a grinding method

Jin Xu, Dasheng Gao, Shuang Cui, Xiaohua Wang and Ningning Liu

### ABSTRACT

Through a simple grinding method, AgI/TiO<sub>2</sub> composites were successfully synthesized. The as-prepared AgI/TiO<sub>2</sub> composites were used as photocatalysts for Rhodamine B (RhB) degradation under visible light irradiation and exhibited excellent photocatalytic performance. In the presence of composites, almost 100% RhB was decomposed after 60 min. The photocatalytic activity of AgI/TiO<sub>2</sub>-0.5 composite was optimal, which was 9.5 times higher than that of pristine TiO<sub>2</sub>, and 15.6 times higher than that of AgI. Moreover, experimental results revealed that the improved photocatalytic activity was not only ascribed to the loading AgI but also resulted from the method that enabled the exposure of more active sites in the composites. In addition, the intimate interfacial contact obtained by this method could also promote the efficient separation of photogenerated electron-hole pairs. Moreover, the possible photocatalytic active species and the stability of the photocatalyst were investigated in detail.

**Key words** | AgI, photocatalysis, rhodamine B, TiO<sub>2</sub>, visible light

Jin Xu  
Dasheng Gao  
Shuang Cui  
Xiaohua Wang  
Ningning Liu (corresponding author)  
College of Chemistry, Chemical Engineering and  
Environmental Engineering,  
Liaoning Shihua University,  
Fushun 113001,  
China  
E-mail: liuningningf@126.com

### INTRODUCTION

Semiconductor photocatalysts with high photocatalytic performance are considered to be one of the most promising materials for solving environmental issues and the energy crisis (Han *et al.* 2018a, 2018b, 2018c). Recently, TiO<sub>2</sub> as a traditional photocatalyst has attracted considerable attention owing to its high efficiency, low cost, non-toxicity and high stability (Fujishima 1972; Chen *et al.* 2012; Dahl *et al.* 2014; Zhang *et al.* 2018). Unfortunately, TiO<sub>2</sub> can only adsorb UV light which accounts for about 4% of the total solar energy, limiting its wide application. To sufficiently utilize solar energy, various strategies including noble metal deposition, doping process, surface sensitization and composite systems have been developed to fabricate efficient TiO<sub>2</sub>-based composite photocatalysts (Kumar & Devi 2011; Wang *et al.* 2014; Chen *et al.* 2017; Gao *et al.* 2018). However, developing the desirable visible light responsive TiO<sub>2</sub>-based composite is still a challenge.

Silver halides are well-known photosensitive materials and are widely employed as source materials in photographic films. As a member of the silver halides, AgI has a smaller band gap than AgCl and AgBr, and it could be considered a promising photocatalyst (Cheng *et al.* 2010). Under ambient condition, there are two main phases of AgI,  $\beta$  and  $\gamma$  phases (Jiang *et al.* 2014).  $\beta$ -AgI as a visible light photocatalyst has become a research hotspot due to its photocatalytic performance for dye degradation. However, AgI could be subject to labile photodecomposition when it is exposed to illumination. It has been reported that the presence of a support (e.g. TiO<sub>2</sub>, Al<sub>2</sub>O<sub>3</sub>, SiO<sub>2</sub>, carbon nanotube (CNT) and g-C<sub>3</sub>N<sub>4</sub>) could stabilize AgI by inhibiting the photographic process (Li *et al.* 2008; Hu *et al.* 2010; Guo *et al.* 2011; An *et al.* 2013; Shi *et al.* 2013; Xu *et al.* 2013; Yi *et al.* 2015; Xia *et al.* 2016; Yang *et al.* 2017). Among these supports, coupling TiO<sub>2</sub> with AgI has

been a subject of intense investigation because of its remarkably high photocatalytic activity in removal of organic dyes under visible light irradiation (Hu et al. 2007; Song et al. 2012; Wang et al. 2015, 2016; Xue et al. 2015; Yang et al. 2016; Yu et al. 2016; Shao et al. 2017). To date, the synthetic methods of fabrication of the AgI/TiO<sub>2</sub> composite are still complicated, high cost and environmentally unfriendly. Thus, it is necessary to develop a simple approach to fabricate the AgI/TiO<sub>2</sub> photocatalyst.

Here, we report that AgI/TiO<sub>2</sub> composites were successfully fabricated through a simple grinding method. The as-prepared AgI/TiO<sub>2</sub> composites were characterized by X-ray diffraction, scanning electron microscopy and UV-Vis spectroscopy. The photocatalytic performance was evaluated by RhB degradation under visible light irradiation. The as-prepared AgI/TiO<sub>2</sub> composites exhibited good visible light absorption and enhanced photocatalytic activities under visible light irradiation. In order to further explain this phenomenon, the photocurrent response properties of photocatalysts were also analyzed. Importantly, possible photocatalytic active species and the stability of the photocatalyst were investigated in detail.

## METHODS

### Chemicals and materials

All chemicals throughout the experiments were analytical grade and used as received from commercial suppliers without further purification. Ethanol (99%) and isopropyl alcohol (99.7%) (IPA) were obtained from Tian Jin Yong Da Chemical Reagent Co., Ltd. Titanium (IV) butoxide and silver nitrate (99.8%) were supplied by Sinopharm Chemical Reagent Co., Ltd. Disodium ethylene diamine tetraacetic acid (EDTA), benzoquinone (BQ) and KI were obtained from Tian Jin Bo Di Chemical Reagent Co., Ltd.

### Preparation of photocatalysts

#### Preparation of TiO<sub>2</sub>

Firstly, 200 mL distilled water was added to a 250 mL beaker, and the pH solution was adjusted to 3 using HNO<sub>3</sub> solution (1 mol L<sup>-1</sup>). A mixture of 20 mL ethanol and 20 mL titanium

(IV) butoxide was added to the above solution. Then, a white suspension was obtained and aged at 70 °C for 48 h. Subsequently, the product was collected by centrifugation and washed thoroughly with water. Finally, the white TiO<sub>2</sub> nanoparticles were collected and dried at 60 °C for 24 h.

### Preparation of AgI

Under dark conditions, AgI nanoparticles were fabricated using a simple precipitation method. Briefly, 0.2 mol L<sup>-1</sup> AgNO<sub>3</sub> aqueous solution (10 mL) was added dropwise into 0.2 mol L<sup>-1</sup> KI (10 mL) aqueous solution under stirring, and then the mixed solution was stirred for 3 h. Afterward, the yellow product was washed with water three times and dried for 24 h.

### Preparation of AgI/TiO<sub>2</sub> composites via a simple grinding method

To obtain the AgI/TiO<sub>2</sub>-0.1 composite, 0.05 g of AgI sample and 0.5 g of TiO<sub>2</sub> were added to a mortar, and the mixture was ground for 15 min. AgI/TiO<sub>2</sub> composites with mass ratio of 0.5:1 (denoted as AgI/TiO<sub>2</sub>-0.5), 1:1 (denoted as AgI/TiO<sub>2</sub>-1) and 2:1 (denoted as AgI/TiO<sub>2</sub>-2) were also fabricated following a similar process. The mass ratio of AgI/TiO<sub>2</sub> composites is listed in Table 1.

### Characterization

The powder X-ray diffractometer (XRD) patterns were carried out on a Rigaku XRD D/max-2500PC instrument with Ni-filtered Cu K $\alpha$  irradiation. UV-Vis diffuse reflectance spectra (UV-Vis DRS) were obtained by a PerkinElmer UV WinLab spectrophotometer with BaSO<sub>4</sub> as a reflectance standard. The product morphologies were analyzed using a SSX-50 scanning electron microscope (SEM; Shimadzu, Japan). Fourier transform infrared (FT-IR) spectra of the samples were

**Table 1** | Mass ratio of AgI/TiO<sub>2</sub> composites

Name	AgI/ (g)	TiO <sub>2</sub> /(g)
AgI/TiO <sub>2</sub> -0.1	0.05	0.5
AgI/TiO <sub>2</sub> -0.5	0.25	0.5
AgI/TiO <sub>2</sub> -1	0.5	0.5
AgI/TiO <sub>2</sub> -2	1.0	0.5

monitored by FT-IR spectrophotometer (VERTEX 70, Bruker, Germany) in the range of 4,000–500 cm<sup>-1</sup> with KBr as reference sample. X-ray photoelectron spectroscopy (XPS, Kratos, ULTRA AXIS DLD) was recorded by a Kratos AXIS Ultra<sup>DLD</sup> system with monochrome Al K $\alpha$  ( $h\nu = 1,486.6$  eV) radiation. Photocurrent measurements were evaluated at a CHI electrochemical workstation (Shanghai). The working electrode was prepared on an ITO glass. Furthermore, 0.2 mol L<sup>-1</sup> of Na<sub>2</sub>SO<sub>4</sub> solution was used as electrolyte.

### Evaluation of photocatalytic activity

The activity of photocatalysts was evaluated by RhB degradation, and the concentration of RhB was determined by the peak at 554 nm with a spectrometer (PerkinElmer UV WinLab spectrophotometer). Typically, 30 mg of photocatalyst powder was mixed with 100 mL of RhB aqueous solution ( $1 \times 10^{-5}$  mol L<sup>-1</sup>) in a quartz reactor (Beijing PerfectLight Technology Co., Ltd, China, <http://www.perfectlight.cn/>) with a water cooling jacket. The cooling jacket was maintained at 5 °C throughout the photocatalysis. Then, the suspension was magnetically stirred in the dark for 60 min to reach adsorption-desorption equilibrium. The suspension was irradiated by a 300 W Xe lamp (Perfect Light PLS-SEX300) with a UV cut filter. The distance between the reactor and light source was 10 cm. At certain time intervals, 3 mL of the specified dispersions was sampled and centrifuged at 8,000 rpm for 5 min. The concentration of the solution was determined by a UV spectrometer. After each cycle of photocatalytic test, the catalysts were recovered. The suspension was centrifuged at 8,000 rpm for 10 min, the obtained catalysts were soaked in ethanol overnight, and then the catalysts were washed with acetone and distilled water three times and dried under vacuum at 60 °C for 24 h.

## RESULTS AND DISCUSSION

### Characterization

AgI/TiO<sub>2</sub> composites with different mass ratio were fabricated via a simple grinding method for 15 min (Figure 1). Figure 2 shows the characteristic morphology of AgI/TiO<sub>2</sub>-0.5 composite. It can be seen from Figure 2 that AgI/TiO<sub>2</sub>-0.5

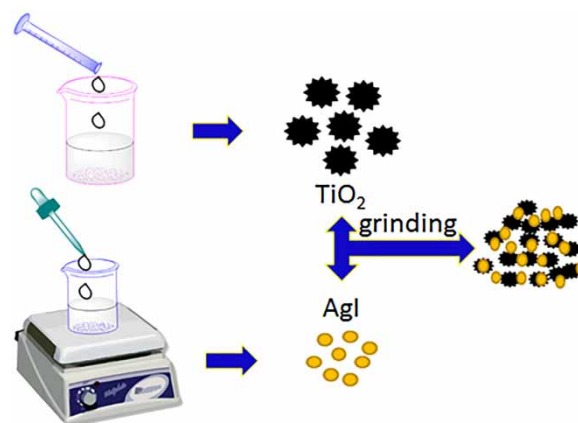


Figure 1 | Illustration of the synthetic route to AgI/TiO<sub>2</sub> composites.

composite displays nonuniform particles, and the size of these particles ranges from several hundred nanometers to several micrometers. The result might be attributed to the grinding method and the introduction of AgI nanoparticles.

Figure 3 shows powder XRD patterns of pristine TiO<sub>2</sub> and AgI/TiO<sub>2</sub> composites. For pristine TiO<sub>2</sub>, the peaks at 25.6°, 38.4°, 48.4°, 54.6° and 62.7° indexed as (101), (004), (200), (211) and (204) reflections associated with anatase TiO<sub>2</sub> (JCPDS no. 21-1272) can be clearly observed. For the sample of AgI/TiO<sub>2</sub> composites, apart from the characteristic peaks of anatase TiO<sub>2</sub>, several new peaks associated with AgI (JCPDS no. 09-0374) can also be observed, indicating the existence of AgI nanoparticles in the samples. Additionally, the peak intensity of TiO<sub>2</sub> decreased, meaning that the AgI content increased gradually in the system.

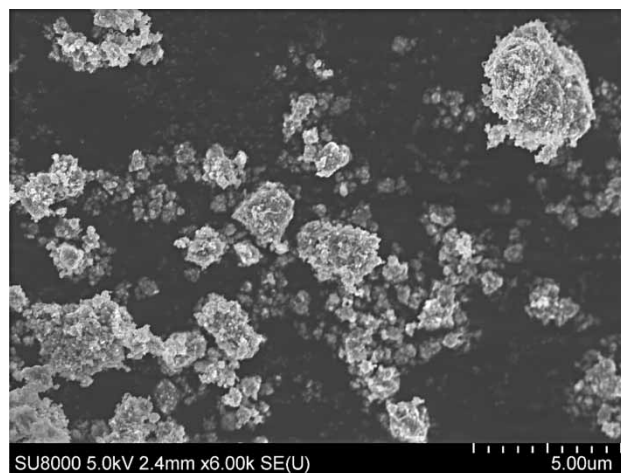
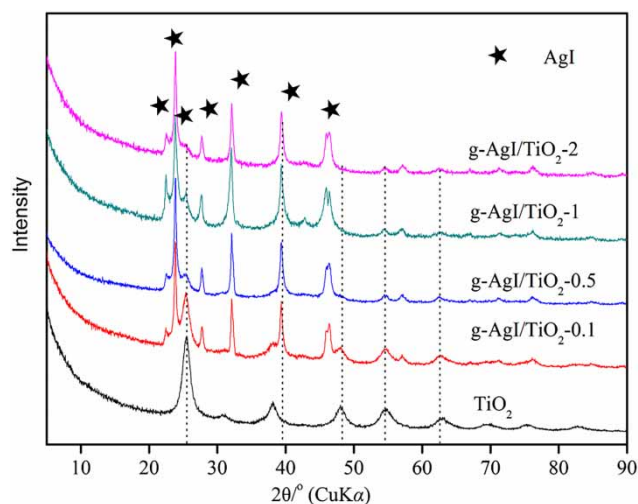


Figure 2 | SEM image of AgI/TiO<sub>2</sub>-0.5 composite.



**Figure 3** | XRD patterns of TiO<sub>2</sub> and AgI/TiO<sub>2</sub> composites.

The nature of species and the chemical states of elements on the surface of AgI/TiO<sub>2</sub>-0.5 composite were obtained by

XPS analysis. As shown in Figure 4(a), the composite is mainly composed of Ti, Ag, I and O elements. Figure 4(b) shows the XPS of Ti 2p region with peaks appearing at 458.5 eV and 464.1 eV. These two peaks are attributed to Ti 2p<sub>1/2</sub> and Ti 2p<sub>3/2</sub> of Ti<sup>4+</sup> in TiO<sub>2</sub>. Two main peaks are observed at the binding energies of around 367.7 eV and 373.7 eV, corresponding to Ag 3d<sub>5/2</sub> and Ag 3d<sub>3/2</sub> (Figure 4(c)), respectively. As for I 3d of AgI/TiO<sub>2</sub>-0.5 composite (Figure 4(d)), two peaks appear at 618.9 eV (3d<sub>5/2</sub>) and 630.4 eV (I 3d<sub>3/2</sub>) and are ascribed to I<sup>-</sup> of AgI. Besides, no peaks corresponding to I<sub>2</sub> and Ag<sup>0</sup> are observed. Thus, it can be confirmed that the AgI/TiO<sub>2</sub> composites were fabricated through the simple grinding method.

The optical absorption property is a significant parameter for a photocatalyst to determine its photocatalytic activity. Figure 5(a) displays the UV-Vis diffuse reflectance spectra of the pristine TiO<sub>2</sub>, AgI and AgI/TiO<sub>2</sub> composites. It can be clearly seen that the pristine TiO<sub>2</sub> shows a broad

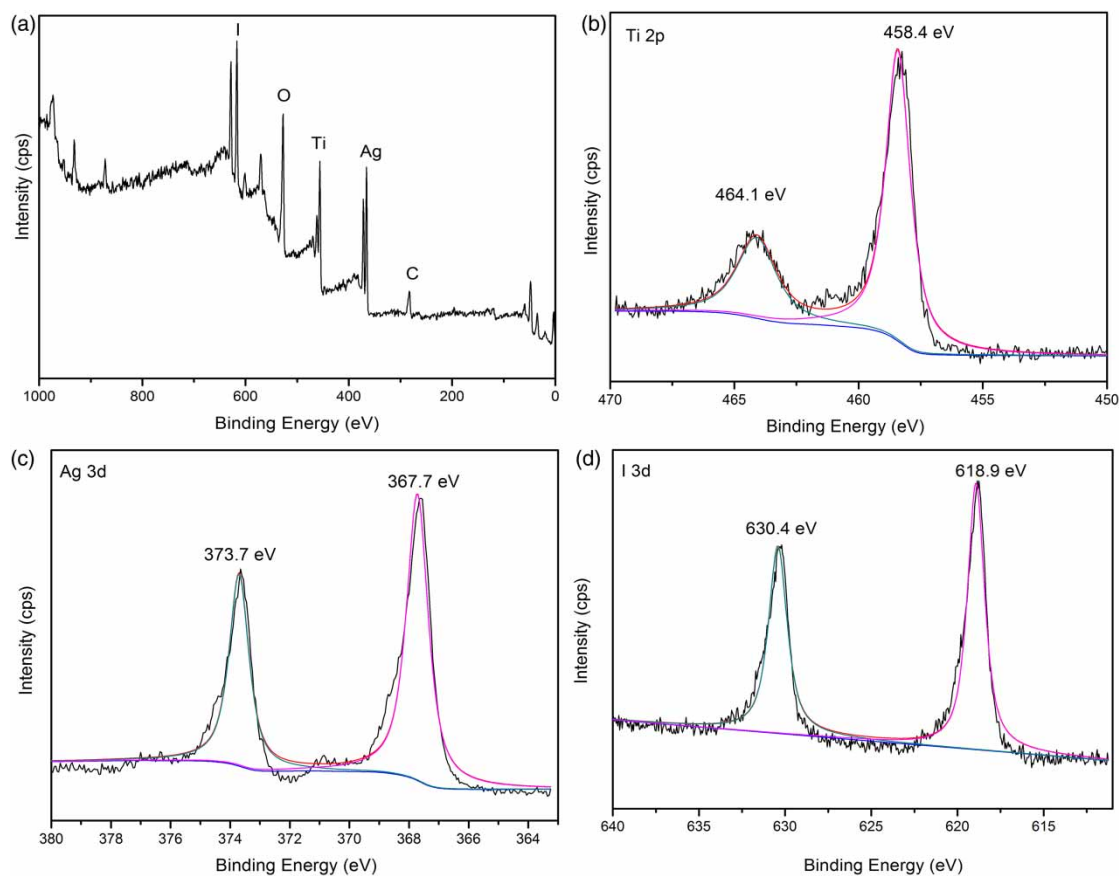


**Figure 4** | XPS patterns of AgI/TiO<sub>2</sub>-0.5 composite.

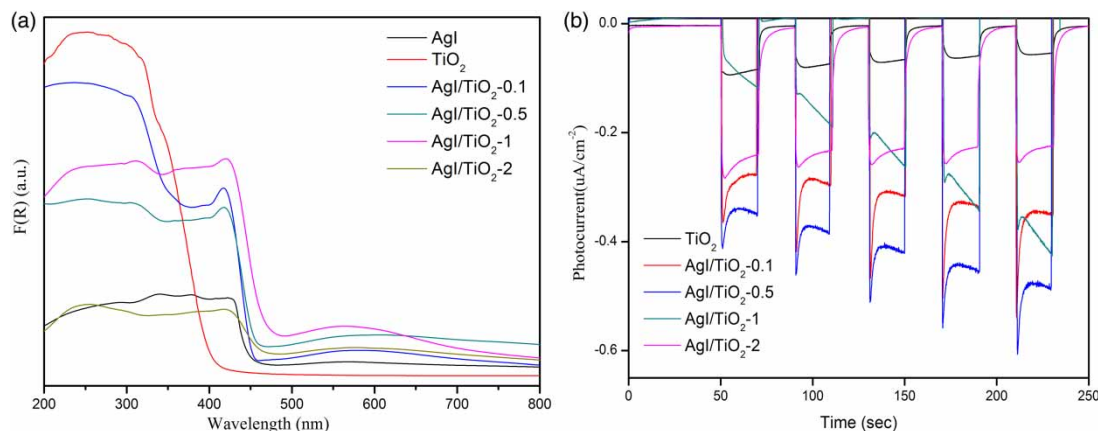


**Figure 5** | (a) UV-Vis spectra of AgI, TiO<sub>2</sub> and AgI/TiO<sub>2</sub> composites; (b) photocurrent response of TiO<sub>2</sub> and AgI/TiO<sub>2</sub> composites.

absorption in the UV region, which is in agreement with a previous report (Yi *et al.* 2015). Compared with the spectra of pristine TiO<sub>2</sub>, the spectra of AgI/TiO<sub>2</sub> composites show a strong broad absorption band in the range of 400 nm to 800 nm. That is, the absorption band of AgI/TiO<sub>2</sub> composites expands to the visible light region (around 425 nm), which is caused by the loading of AgI nanoparticles.

To evaluate the efficient separation of photogenerated electron-hole pairs, photocurrent experiments were carried out under visible light irradiation. As illustrated in Figure 5(b), the photocurrent density on AgI/TiO<sub>2</sub> composites is higher than that on the pristine TiO<sub>2</sub>, indicating that the loading of AgI leads to the enhancement of visible light response. It is clear from Figure 5(b) that the highest photocurrent density is observed on the AgI/TiO<sub>2</sub>-0.5 composite, indicating its highest photocatalytic activity among these catalysts. Therefore, the result suggests that these

photogenerated electron-hole pairs could be efficiently separated in this system under visible light irradiation.

### Photocatalytic degradation of RhB

In order to evaluate the photocatalytic activities of different catalysts, RhB degradation experiments were carried out under visible light irradiation. Before irradiation, all photocatalysts in the RhB solution were stirred in the dark for 60 min to reach adsorption-desorption equilibrium. As shown in Figure 6(a), about 6.8% and 7.6% of RhB molecules were adsorbed onto the pristine TiO<sub>2</sub> and AgI, respectively. However, the adsorption capacities of AgI/TiO<sub>2</sub> composites are higher than those of pristine TiO<sub>2</sub> and AgI. About 11.4%, 31.3%, 19.2% and 19.7% of RhB molecules were adsorbed on the surface of AgI/TiO<sub>2</sub>-x (0.1, 0.5, 1, 2) composites, respectively. The discrepancy in the adsorption could be

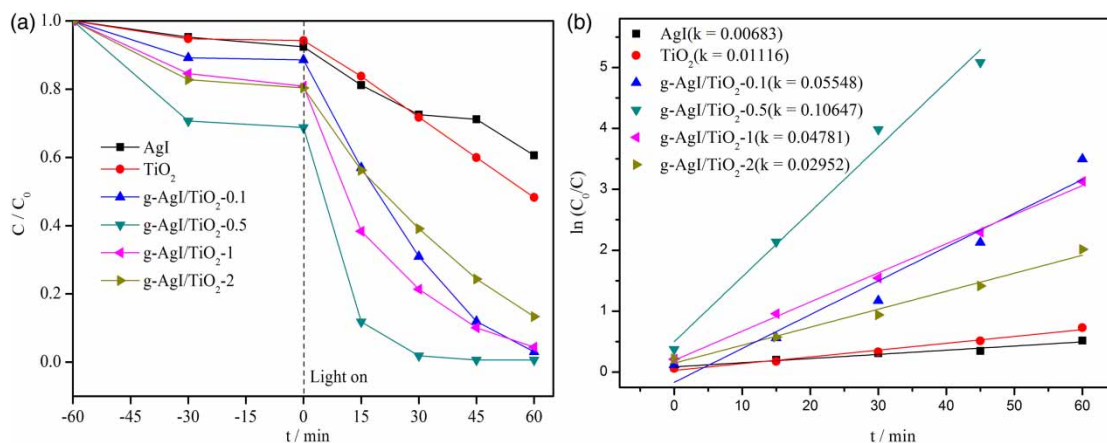


**Figure 6** | (a) Photocatalytic performance for RhB degradation over AgI, TiO<sub>2</sub> and AgI/TiO<sub>2</sub> composites under visible light irradiation; and (b) their reaction rate constants (k).

caused by different surface area and different 'chemical affinity' for the pristine TiO<sub>2</sub>, AgI and AgI/TiO<sub>2</sub> composites. As the reaction proceeded, all catalysts showed non-negligible photocatalytic performance for RhB degradation. However, the photocatalytic activities of AgI/TiO<sub>2</sub> composites showed high activity, and RhB was almost completely decomposed in 60 min. It is found that AgI/TiO<sub>2</sub>-0.5 composite displayed the highest photocatalytic activity and its degradation efficiency reached almost 100% within 45 min. To further confirm the above results, the degradation kinetics equation was used to describe the process of photocatalytic reaction. The function of  $\ln(C/C_0)$  versus time ( $t$ ) is a linear relationship, indicating that the process of RhB degradation follows the pseudo-first-order reaction kinetics model:

$$-\frac{d(C/C_0)}{dt} = kt$$

where  $C_0$  is the initial concentration of RhB before irradiation,  $C$  is the concentration of RhB at  $t$  time, and  $k$  is a rate constant. As demonstrated in Figure 6(b), comparison of the rate constants for RhB degradation over the catalysts reveals a similar trend as discussed previously. The photocatalytic activity of AgI/TiO<sub>2</sub> composite rose with the increasing mass ratio of AgI and TiO<sub>2</sub> from 0.1:1 to 0.5:1, which might be attributed to the increased number of active sites in the AgI/TiO<sub>2</sub> composite. However, when the AgI loading mass is greater than or equal to 1:1, the photocatalytic activity decreased. A possible reason might be that excessive AgI could not sufficiently contact with TiO<sub>2</sub>, so that the formation of intimate interfacial contact is difficult. In addition, the excessive AgI might aggregate on the catalyst surface to reduce the available active sites, resulting in the decrease in photocatalytic activity. Therefore, the optimum AgI content in the composite is 0.5:1. The rate constants of AgI/TiO<sub>2</sub>-0.5 composite for RhB degradation are 9.5 and 15.6 times higher than those of pristine TiO<sub>2</sub> and AgI, respectively.

### Possible photocatalytic mechanism

To give further evidence to the role of active species under visible light, the main reactive species including  $\cdot\text{OH}$ ,  $\cdot\text{O}_2^-$ , and  $\text{h}^+$  were investigated during the photocatalysis process.

Isopropanol (IPA), disodium ethylene diamine tetraacetic acid (EDTA) and benzoquinone (BQ) were applied as scavengers of  $\cdot\text{OH}$ ,  $\text{h}^+$  and  $\cdot\text{O}_2^-$ , respectively. As shown in Figure 7(a), the degradation efficiency of RhB significantly decreased in the presence of BQ. Since BQ is a  $\cdot\text{O}_2^-$  quencher,  $\cdot\text{O}_2^-$  could be one of the main active species during the photocatalysis process. However, the presence of IPA and EDTA did not cause obvious changes in the RhB degradation efficiency, suggesting that  $\cdot\text{OH}$  and  $\text{h}^+$  do not play an important role in the photocatalytic process. Thus,  $\cdot\text{O}_2^-$  is the main active species during the RhB degradation process.

### Stability and reusability of AgI/TiO<sub>2</sub>-0.5 composite

Figure 7(b) shows the stability of AgI/TiO<sub>2</sub>-0.5 composite for RhB degradation under visible light irradiation. AgI/TiO<sub>2</sub>-0.5 composite was easily recycled by simple centrifugation and ethanol treatment in these recycling experiments. After five cycles, the photocatalytic activity did not decrease significantly in the RhB degradation under visible light irradiation. The results demonstrate that AgI/TiO<sub>2</sub>-0.5 composite is an effective and stable photocatalyst during the degradation process. However, we find that the color of spent AgI/TiO<sub>2</sub>-0.5 composite changes from yellow to grey, indicating the occurrence of AgI decomposition. To further confirm the result, the spent AgI/TiO<sub>2</sub>-0.5 composite collected after five cycles was analyzed by XRD. XRD patterns in Figure 7(c) show that several new peaks are observed in the spent samples. These new peaks are consistent with Ag<sup>0</sup> species (JCPDS no. 04-0783). Therefore, it is confirmed that the AgI content in the composite might slightly decrease after five cycles.

### CONCLUSIONS

In summary, AgI/TiO<sub>2</sub> composite photocatalysts were synthesized by a simple grinding process. The as-prepared AgI/TiO<sub>2</sub> composites were used as photocatalysts for RhB degradation under visible light irradiation and exhibited excellent photocatalytic performance. The enhanced photocatalytic activity was not only attributed to the loading AgI but also resulted from the method that enabled the exposure

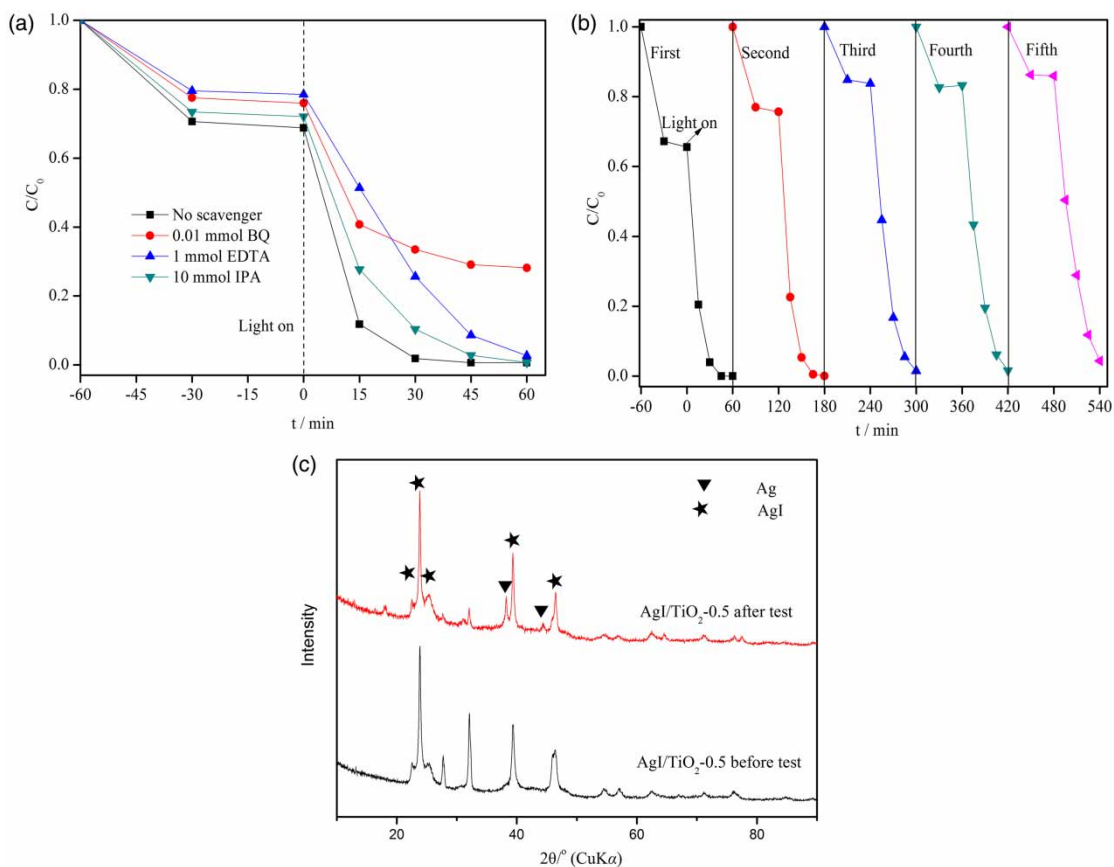


**Figure 7** | (a) Effects of different scavengers over AgI/TiO<sub>2</sub>-0.5 composite for RhB degradation; (b) reusability of AgI/TiO<sub>2</sub>-0.5 composite for RhB degradation; (c) comparison of XRD patterns of AgI/TiO<sub>2</sub>-0.5 composite before and after photocatalytic test.

of more active sites in the composites. In addition, the intimate interfacial contact obtained by this method could also promote the efficient separation of photogenerated electron-hole pairs. The photocatalytic mechanism demonstrated that the  $\cdot\text{O}_2^-$  was the dominant active species during the photocatalytic process. Moreover, the photocatalytic activity of AgI/TiO<sub>2</sub> composite could still remain after four cycles, indicating the potential application in wastewater treatment. This work may offer an efficient way for large-scale synthesis of high-efficiency, visible light photocatalysts.

## ACKNOWLEDGEMENTS

This work was supported by the National Natural Science Foundation of China (Grants: 41773093 and 51704151).

## REFERENCES

- An, C., Jiang, W., Wang, J., Wang, S., Ma, Z. & Li, Y. 2013 Synthesis of three-dimensional AgI@TiO<sub>2</sub> nanoparticles with improved photocatalytic performance. *Dalton Transactions* **42**, 8796–8801.
- Chen, H., Nanayakkara, C. E. & Grassian, V. H. 2012 Titanium dioxide photocatalysis in atmospheric chemistry. *Chemical Reviews* **112**, 5919–5948.
- Chen, L. M., Gu, Q., Hou, L. X., Zhang, C. Q., Lu, Y. B., Wang, X. X. & Long, J. L. 2017 Molecular p–n heterojunction-enhanced visible-light hydrogen evolution over a N-doped TiO<sub>2</sub> photocatalyst. *Catalysis Science & Technology* **7**, 2039–2049.
- Cheng, H., Huang, B., Dai, Y., Qin, X. & Zhang, X. 2010 One-step synthesis of the nanostructured AgI/BiOI composites with highly enhanced visible-light photocatalytic performances. *Langmuir* **26**, 6618–6624.
- Dahl, M., Liu, Y. & Yin, Y. 2014 Composite titanium dioxide nanomaterials. *Chemical Reviews* **114**, 9853–9889.

- Fujishima, A. 1972 Electrochemical photolysis of water at a semiconductor electrode. *Nature* **238**, 37–38.
- Gao, D. S., Liu, N. N., Li, W. W. & Han, Y. D. 2018 Fabrication of nanoporous polymeric crystalline TiO<sub>2</sub> composite for photocatalytic degradation of aqueous organic pollutants under visible light irradiation. *Applied Organometallic Chemistry* **32**, e4119.
- Guo, J. F., Ma, B., Yin, A., Fan, K. & Dai, W. L. 2011 Photodegradation of rhodamine B and 4-chlorophenol using plasmonic photocatalyst of Ag–AgI/Fe<sub>3</sub>O<sub>4</sub>@SiO<sub>2</sub> magnetic nanoparticle under visible light irradiation. *Applied Catalysis B* **101**, 580–586.
- Han, Y. D., Bai, C. P., Zhang, L. X., Wu, J. B., Meng, H., Xu, J. L., Xu, Y., Liang, Z. Q. & Zhang, X. 2018a A facile strategy for fabricating AgI–MIL-53(Fe) composites: superior interfacial contact and enhanced visible light photocatalytic performance. *New Journal of Chemistry* **42**, 3799–3807.
- Han, Y. D., Shi, H. L., Bai, C. P., Zhang, L. X., Wu, J. B., Meng, H., Xu, Y. & Zhang, X. 2018b Ag<sub>3</sub>PO<sub>4</sub>–MIL-53(Fe) composites with visible-light-enhanced photocatalytic activities for Rhodamine B degradation. *Chemistry Select* **3**, 8045–8050.
- Han, Y. D., Zhang, L. X., Bai, C. P., Wu, J. B., Meng, H., Xu, Y., Liang, Z. Q., Wang, Z. P. & Zhang, X. 2018c Fabrication of AgI/MIL-53(Fe) composites with enhanced photocatalytic activity for Rhodamine B degradation under visible light irradiation. *Applied Organometallic Chemistry* **32**, e4325.
- Hu, C., Guo, J., Qu, J. & Hu, X. 2007 Photocatalytic degradation of pathogenic bacteria with AgI/TiO<sub>2</sub> under visible light irradiation. *Langmuir* **23**, 4982–4987.
- Hu, C., Peng, T., Hu, X., Nie, Y., Zhou, X., Qu, J. & He, H. 2010 Plasmon-induced photodegradation of toxic pollutants with Ag–AgI/Al<sub>2</sub>O<sub>3</sub> under visible-light irradiation. *Journal of the American Chemical Society* **132**, 857–862.
- Jiang, W., An, C., Liu, J., Wang, S., Zhao, L., Guo, W. & Liu, J. 2014 Facile aqueous synthesis of β-AgI nanoplates as efficient visible-light-responsive photocatalyst. *Dalton Transactions* **43**, 300–305.
- Kumar, S. G. & Devi, L. G. 2011 Review on modified TiO<sub>2</sub> photocatalysis under UV/visible light: selected results and related mechanisms on interfacial charge carrier transfer dynamics. *The Journal of Physical Chemistry A* **115**, 13211–13241.
- Li, Y., Zhang, H., Guo, Z., Han, J., Zhao, X., Zhao, Q. & Kim, S. J. 2008 Highly efficient visible-light-induced photocatalytic activity of nanostructured AgI/TiO<sub>2</sub> photocatalyst. *Langmuir* **24**, 8351–8357.
- Shao, Y. Y., Ye, W. D., Sun, C. Y., Liu, C. L. & Wang, Q. 2017 Visible-light-induced degradation of polybrominated diphenyl ethers with AgI–TiO<sub>2</sub>. *RSC Advances* **7**, 39089–39095.
- Shi, H., Chen, J., Li, G., Nie, X., Zhao, H., Wong, P. K. & An, T. 2013 Synthesis and characterization of novel plasmonic Ag/AgX–CNTs (X = Cl, Br, I) nanocomposite photocatalysts and synergetic degradation of organic pollutant under visible light. *ACS Applied Materials & Interfaces* **5**, 6959–6967.
- Song, S., Hong, F., He, Z., Cai, Q. & Chen, J. 2012 AgIO<sub>3</sub>-modified AgI/TiO<sub>2</sub> composites for photocatalytic degradation of p-chlorophenol under visible light irradiation. *Journal of Colloid and Interface Science* **378**, 159–166.
- Wang, H., Zhang, L., Chen, Z., Hu, J., Li, S., Wang, Z., Liu, J. & Wang, X. 2014 Semiconductor heterojunction photocatalysts: design, construction, and photocatalytic performances. *Chemical Society Reviews* **43**, 5234–5244.
- Wang, Q., Chen, M., Zhu, N., Shi, X., Jin, H., Zhang, Y. & Cong, Y. 2015 Preparation of AgI sensitized amorphous TiO<sub>2</sub> as novel high-performance photocatalyst for environmental applications. *Journal of Colloid and Interface Science* **448**, 407–416.
- Wang, Q., Shi, X., Xu, J., Crittenden, J. C., Liu, E., Zhang, Y. & Cong, Y. 2016 Highly enhanced photocatalytic reduction of Cr(VI) on AgI/TiO<sub>2</sub> under visible light irradiation: influence of calcination temperature. *Journal of Hazardous Materials* **307**, 213–220.
- Xia, D., Hu, L., Tan, X., He, C., Pan, W., Yang, T., Huang, Y. & Shu, D. 2016 Immobilization of self-stabilized plasmonic Ag–AgI on mesoporous Al<sub>2</sub>O<sub>3</sub> for efficient purification of industrial waste gas with indoor LED illumination. *Applied Catalysis B* **185**, 295–306.
- Xu, H., Yan, J., Xu, Y., Song, Y., Li, H., Xia, J., Huang, C. & Wan, H. 2015 Novel visible-light-driven AgX/graphite-like C<sub>3</sub>N<sub>4</sub> (X = Br, I) hybrid materials with synergistic photocatalytic activity. *Applied Catalysis B* **129**, 182–193.
- Xue, B., Sun, T., Wu, J. K., Mao, F. & Yang, W. 2015 AgI/TiO<sub>2</sub> nanocomposites: ultrasound-assisted preparation, visible-light induced photocatalytic degradation of methyl orange and antibacterial activity. *Ultrasonics Sonochemistry* **22**, 1–6.
- Yang, L., Gao, M., Dai, B., Guo, X., Liu, Z. & Peng, B. 2016 Synthesis of spindle-shaped AgI/TiO<sub>2</sub> nanoparticles with enhanced photocatalytic performance. *Applied Surface Science* **386**, 337–344.
- Yang, L., An, Y., Dai, B., Guo, X., Liu, Z. & Peng, B. 2017 Fabrication of carbon nanotube-loaded TiO<sub>2</sub>@AgI and its excellent performance in visible-light photocatalysis. *Korean Journal of Chemical Engineering* **34**, 476–483.
- Yi, J., Huang, L., Wang, H., Yu, H. & Peng, F. 2015 AgI/TiO<sub>2</sub> nanobelts monolithic catalyst with enhanced visible light photocatalytic activity. *Journal of Hazardous Materials* **284**, 207–214.
- Yu, D., Bai, J., Liang, H., Ma, T. & Li, C. 2016 Fabrication of AgI–TiO<sub>2</sub> loaded on carbon nanofibers and its excellent recyclable and renewable performance in visible-light catalysis. *Journal of Molecular Catalysis A: Chemical* **420**, 1–10.
- Zhang, L., Chen, P., Wang, J., Li, H., Sun, W. & Yan, P. 2018 Anthracene-decorated TiO<sub>2</sub> thin films with the enhanced photoelectrochemical performance. *Journal of Colloid and Interface Science* **530**, 624–630.